22 October 1999

ELSEVIER

Chemical Physics Letters 312 (1999) 108–114

CHEMICAL PHYSICS LETTERS

www.elsevier.nl/locate/cplett

Dissociative photoionization dynamics of SF_6 by ion imaging with synchrotron undulator radiation

Darcy S. Peterka [a], Musahid Ahmed [a], Cheuk-Yiu Ng [b], Arthur G. Suits [a,*]

[a] *Chemical Sciences Division, Ernest Orlando Lawrence Berkeley National Laboratory, Berkeley, CA 94720, USA*

[b] *Ames Laboratory, United States Department of Energy, and Department of Chemistry, Iowa State University, Ames, IA 50011, USA*

Received 2 May 1999; in final form 3 August 1999

Abstract

The technique of photofragment imaging, widely used in the study of neutral photochemistry, has been adapted to use on a vacuum ultraviolet undulator beamline at the advanced light source, affording a new approach to the study of dissociative ionization processes. The technique allows direct inversion of the raw data to yield angular and translational energy distributions for the product ions. The method is applied here to study the dissociative ionization of SF_6 at photon energies from 15 to 28 eV. The experiment allows for detailed characterization of the angular and translational energy distributions of the fragments, providing insight into the decay mechanisms of these excited ionic states.

1. Introduction

The oscillator strength distribution of most molecules reaches a maximum in the vacuum ultraviolet (VUV) [1], and dissociative ionization is the principle decay mechanism following excitation of molecules in the VUV. Dissociative ionization is thus one of the most important photochemical processes. Dissociative ionization processes can illuminate features of ion–molecule reactions just as neutral photodissociation has been used to characterize some reactions in so-called 'half-collision' experiments. Sophisticated approaches have been employed in recent years using coincidence methods [2,3], for example, to study dissociative ionization from energy-selected ions. In general, these methods rely on analysis of the ion time-of-flight (TOF) peak shape to characterize the kinetic energy released as well as the angular distributions for the process. These approaches achieve a precise definition of the initial state of the ion, but generally do not yield the full kinetic energy or angular distributions for the process of interest. We have recently adapted the ion imaging technique [4] for use on the chemical dynamics beamline, an undulator beamline at the advanced light source [5].

Ion imaging is a method that has recently seen wide application in neutral photochemistry, crossed-beam collision dynamics and reactive scattering [6]. The technique has the advantage that complete energy and angular distributions are recorded simultaneously, and the data analysis may be accomplished by direct inversion of the raw data. A closely related technique has been used by Eland and coworkers in a coincidence mode to look at three-body fragmenta-

* Corresponding author. Fax: +1-510-486-5311; e-mail: agsuits@lbl.gov

0009-2614/99/$ - see front matter
PII: S0009-2614(99)00918-5

tion processes in double ionization [7,8]. In this first application of the ion imaging technique in conjunction with synchrotron radiation, the 'white beam' from the undulator is used with its inherent 2% bandwidth.

Studies of SF_6 dissociative ionization include early photoionization mass spectrometry measurements of partial ionization cross-sections using both a helium continuum source [9] and synchrotron radiation [10] as well as electric dipole $(e,e+\text{ion})$ spectroscopy [11]. In addition, an early photoelectron–photoion coincidence (PEPICO) study reported kinetic energy release for SF_6 through the $\tilde{X}$ and $\tilde{A}$ states [12]. More recent studies have included negative ion mass spectrometry [13], and both low- [14] and high-resolution [15] PEPICO studies using synchrotron radiation. In the PEPICO study of Creasey et al., detailed dynamical information was inferred from average kinetic energy release measurements for SF_5^+, SF_4^+ and SF_3^+ as well as onsets for the specific decay channels [14] Evans et al. [15], using a supersonic molecular beam of SF_6 with a 6.65 m Eagle monochromator, measured high-resolution PEPICO TOF spectra for fragment ions from SF_6 dissociative ionization, with particular interest in the thermochemistry. Recently, Yencha et al. reported a high-resolution threshold photoelectron spectroscopy study for SF_6 to 28 eV [16]. In this Letter, we present preliminary results obtained on an imaging endstation on the chemical dynamics beamline, characterizing the dissociative photoionization dynamics of SF_6 in a molecular beam, excited at energies from 15 to 28 eV.

2. Experimental

The experiments were performed in a new endstation recently added to the chemical dynamics beamline. The apparatus is schematically illustrated in the inset to Fig. 1. Briefly, it features a molecular beam source pumped by a 2000 l/s magnetic bearing turbomolecular pump. The molecular beam is skimmed once before entering the ionization chamber, pumped by two 400 l/s magnetic bearing turbomolecular pump. Product ions are accelerated by

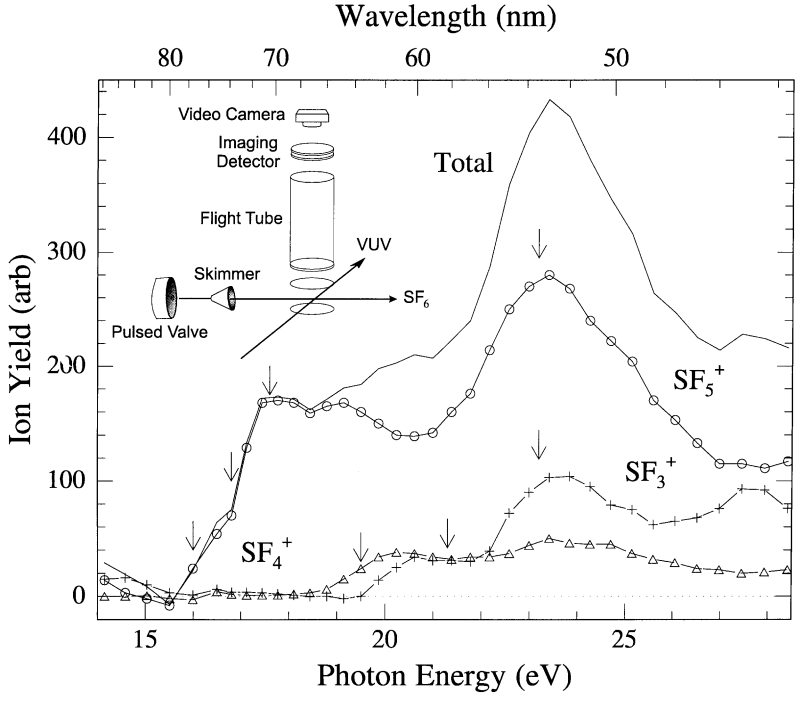

Fig. 1. Photoion yield spectra for SF_6. Inset shows a schematic view of the imaging endstation.

repeller and acceleration fields into a 0.5 m flight tube perpendicular to the plane of the beams. They then strike a position-sensitive detector, which is a 40-mm-diameter dual microchannel plate coupled to a phosphor screen (Galileo 3040FM). Photionization yield (PIY) spectra were obtained by integrating the ion TOF peaks as a function of photon energy. Mass-selected images were obtained by pulsing the microchannel plate, typically pulsing from a DC value of −1100 to −1900 V, with 300 ns duration. The detector is viewed by an integrating fast-scan video camera system employing thresholding in conjunction with a linear video look-up table. Typical accumulation times were 10 min for each image.

The molecular beam was produced by passing neat SF_6 through a piezoelectric pulsed valve operating at 90 Hz with 100 μs pulses. TOF mass spectra were recorded by placing a photomultiplier tube to view the detector. The polarization of the undulator radiation is purely linear, and parallel to the plane of the detector. The images recorded are 2-dimensional projections of the 3-dimensional recoiling product ion sphere. The translational energy, speed and angular distributions were reconstructed from the projection using standard techniques [6].

Images of SF_5^+, SF_4^+ and SF_3^+ were recorded (when observed) at various photon energies from to 16.0 to 24 eV. These are not coincidence experiments, and the dissociation processes are not presented for energy-selected ions. However, to estimate contributions from particular electronic states, difference images were generated for SF_5^+ during analysis. This involved collecting two images one below and one above the rise of a feature in the PIY curve and then subtracting them. This approach is intended to provide an overview of the dynamics in a given region, roughly corresponding to a threshold experiment, but clearly it is not a truly energy-selected measurement. Analysis of all the images were performed using the conventional inverse Abel transform to reconstruct the product-flux contour maps from the images, which are 2-dimensional projections of the 3-dimensional fragment distributions. The reconstructed images were then integrated over the angular distribution as a function of recoil speed to generate the speed distributions, and integrated radially as a function of polar angle to yield the angular distributions.

3. Results

3.1. PIY spectra

The PIY spectra for the various product ions are shown in Fig. 1. Arrows in the figure indicate photon energies at which images were recorded to obtain

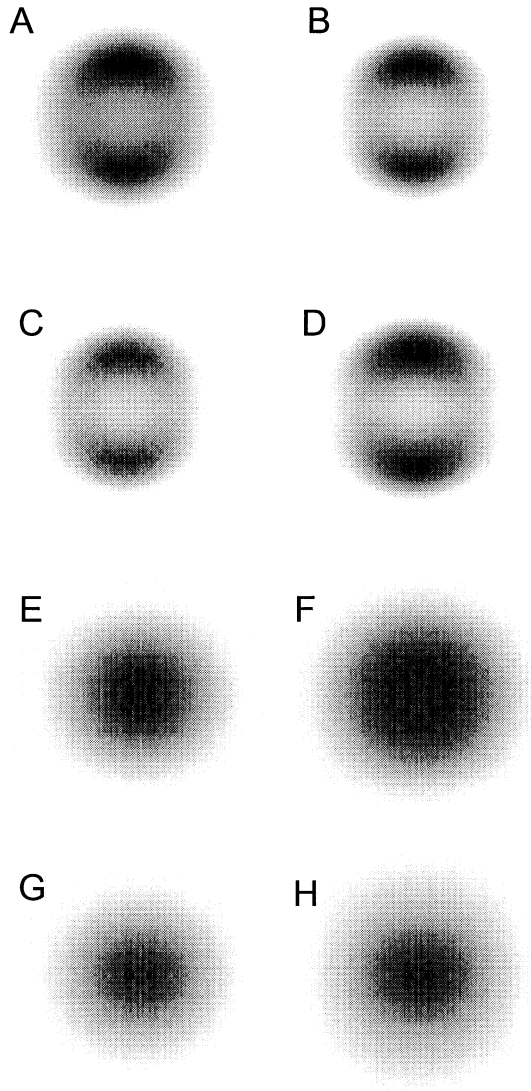

Fig. 2. (A)–(D): SF_5^+ data images at the indicated photon energy. (A) 16 eV. (B) 16.8–16 eV. (C) 17.6–16.8 eV. (D) 23.2–21.3 eV. (E)–(H) Data images for the following product ion and photon energy: (E) SF_4^+ 19.5 eV, (F) SF_4^+ 21.3 eV, (G) SF_3^+ 21.3 eV, (H) SF_3^+ 23.2 eV.

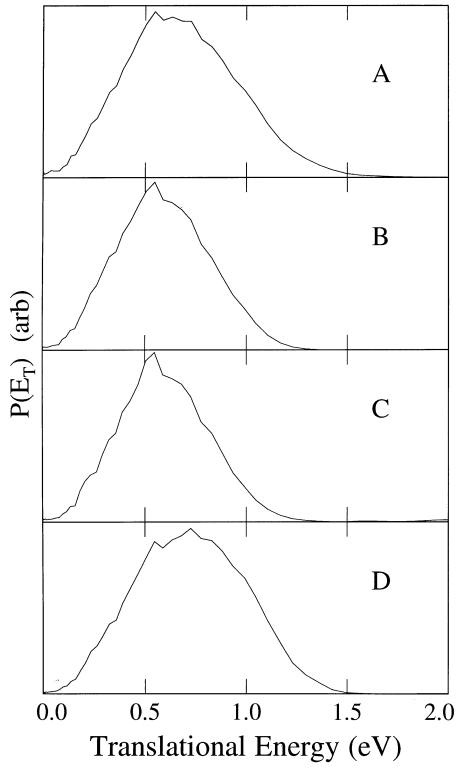

Fig. 3. Total translational energy distributions for the images shown in Fig. 2A–D.

translational energy and angular distributions. The onset for SF_5^+ is found near 15.5 eV, consistent with previous reports (see Ref. [17] and references therein). It shows additional onsets at 17 eV, 20 eV, some decrease beginning near 19 eV, and a very prominent resonant feature at 23 eV. SF_4^+ shows an onset around 18.5 eV, again consistent with previous reports, and shows only modest changes up to 30 eV. SF_3^+ appears at 20 eV, and exhibits the same resonant feature seen in SF_5^+ near 23 eV.

3.2. SF_5^+

An image for SF_5^+ at 16 eV, and difference images at 16.8, 17.6, and 23.2 eV are shown in Fig. 2A–D. From these images, we obtain the translational energy distributions shown in Fig. 3. These energy distributions show surprisingly little change with the changing excitation energy throughout this region. As mentioned above, these results are not obtained for energy-selected ions. Instead, we derive the translational energy distributions from difference images taken in an effort to isolate the contribution for a given region of onset. At 16 eV the average translational energy release is 0.62 eV, and extends to a maximum of 1.8 eV. At 16.8 and 17.6 eV the average release is ~ 0.55 eV with a maximum energy of 1.4 eV, while at 23.2 eV the average energy release is 0.66 eV with a maximum release of ~ 1.7 eV.

The angular distributions are shown for SF_5^+ for the four representative photon energies in Fig. 4. These were fitted to the familiar expression: $I(\Theta) \propto 1 + \beta P_2[\cos(\Theta)]$ to obtain the β parameters [18]. The β values obtained are: 0.94 at 16 eV, 1.23 at

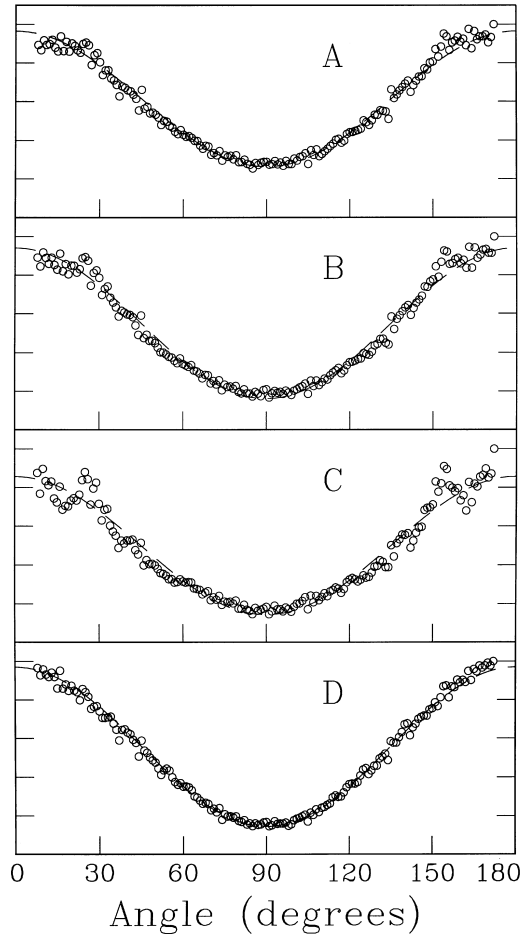

Fig. 4. Angular distributions obtained from the images in Fig. 2A–D.

16.8 eV, 1.24 at 17.6 eV, and reach a maximum of 1.31 at 23.2 eV.

3.3. SF_4^+ and SF_3^+

Images recorded for SF_4^+ at 19.5 and 21.3 eV and SF_3^+ at 21.3 and 23.2 eV are shown in Fig. 2E–H. The thresholds for SF_4^+ and SF_3^+ production are around 18.5 and 19 eV, respectively, consistent with previous reports. Since the co-fragments are not necessarily known, we present recoil speed distributions rather than total translational energy distributions. These are shown in Fig. 5, along with that obtained for SF_5^+ at 16 eV for comparison. The corresponding angular distributions (not shown) are nearly isotropic for both SF_4^+ and SF_3^+ as can be seen in the data images.

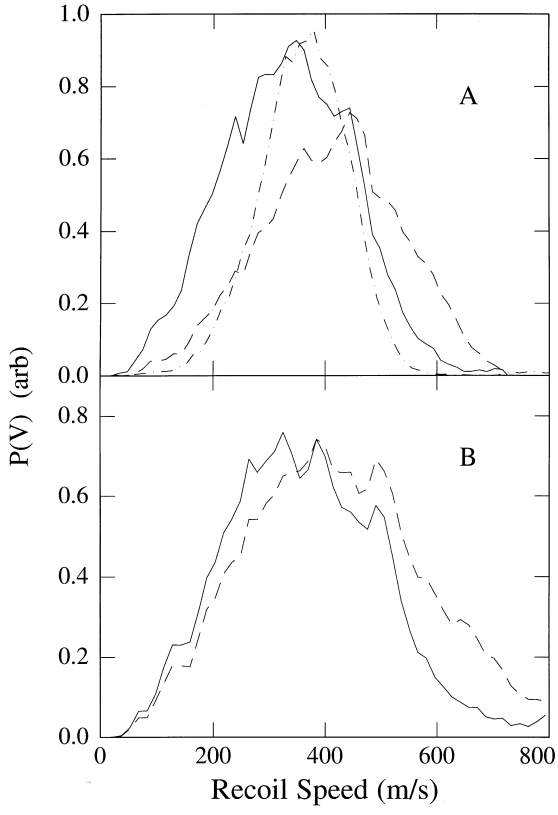

Fig. 5. Recoil speed distributions for the following fragments and photon energies: (A) solid line, SF_4^+ 19.5 eV; dashed line, SF_4^+ 21.3 eV; dot-dashed line, SF_5^+ 16 eV; (B) solid line, SF_3^+ 21.3 eV; dashed line, SF_3^+ 23.2 eV.

4. Discussion

The use of difference images allows us to discuss the dynamics in the language of a threshold measurement; that is, if the photoion yield spectrum is constant over some region, then the difference images would vanish in that region and we speak of the 'absence' of the ion in that region. This is justified owing to the correspondence between the threshold photoelectron spectrum and the structure in the PIY spectra, but it only reliable where a large increase in the yield of a particular ion is observed, and it fails entirely in the region of the shape resonance (see below) where autoionization dominates, giving rise to energetic electrons.

Previous studies of the PIY spectra for SF_6 were mainly conducted up to the He(I) line at 21.2 eV [9], and our results are largely consistent with that previous work. More recently, Mitsuke et al. [13], reported PIY measurements for SF_5^+ and SF_3^+ up to 31 eV in the course of studies of ion–pair formation. The dominant feature that appears in the energy range from 21 to 30 eV is the broad resonance evident in both the SF_5^+ and SF_3^+. This feature is not seen as prominently in the SF_4^+ ion. It is believed that this feature represents a shape resonance arising from excitation to quasibound levels of the electron that are briefly trapped by a barrier formed from the electron density around the electronegative fluorine atoms [19]. Mitsuke et al. argue that this resonance is associated with a $5a_{1g} \rightarrow 6t_{1u}$ transition, which correlates to a $3s \rightarrow 3p$ transition on the central sulfur atom. The translational energy distributions for SF_5^+ at this photon energy imply that much of the additional energy is taken away by the electron in the process of autoionization (otherwise the energy would exceed that permitting bound SF_5^+). Studying relying on coincidence with threshold electrons show no evidence of this feature [16,20], supporting the inference that it is associated with autoionization to lower lying ionic states.

The detailed kinetic energy distributions shown in Fig. 3 are the first obtained for dissociative photoionization of SF_6, and noteworthy in the level of detail achieved. The average of the distributions agree reasonably well with the low-resolution measurements previously reported [14,17]. These distributions are remarkably independent of ionization en-

ergy, possibly suggesting a late barrier to decomposition of SF_6^+ to $SF_5^+ + F$. Consideration of the geometry changes involved provides a plausible picture of the dissociation pathway. Stretching of one of the S–F bonds in SF_6^+ yields an SF_5^+ ion initially in a square pyramidal geometry [12]. However, recent ab initio calculations [21,22] confirm that the structure of SF_5^+ is clearly trigonal bipyramidal (D_{3h}), so that extensive rearrangement must occur during the dissociation process. The kinetic energy release likely reflects fairly efficient conversion of the energy of this barrier into product repulsion. The fact that the kinetic energy distributions are similar for several excited states of the SF_6^+ ion may indicate that internal conversion to the ground state of the ion precedes dissociation. This is also consistent with the similarities in the angular distributions.

The angular distributions in the figures represent the first at this level of detail for a dissociative ionization event, although Powis and coworkers [23,24] have investigated these and related phenomena through examination of ion TOF peak shapes. Our observed anisotropic SF_5^+ angular distributions augment the picture of the dynamics sketched above. All of the SF_5^+ distributions show considerable anisotropy consistent with a parallel dissociation; that is, the fragments show a strong tendency to dissociate on an axis parallel to the polarization of the VUV radiation. This may seem surprising for such a highly symmetrical molecule (point group O_h.) Ionization through the $\tilde{X}$, $\tilde{A}$ and $\tilde{B}$ states of SF_6^+ are $(1t_{1g}^{-1})$ and $[(5t_{1u}^{-1}) + (1t_{2u}^{-1})]$ ionizations respectively [17]. These all represent removal of 2p lone-pair electrons from the fluorine atoms [9], so it is perhaps not so surprising that a more local view of the ionization and subsequent dissociation is appropriate. The angular distributions further show that the autoionization via the shape resonance must be very rapid. Photoelectron spectra at these photon energies would be useful to identify the SF_6^+ state(s) formed in the ionization step. All of these angular distributions show that the SF_6^+ dissociation is very rapid, occurring on a timescale short compared to its rotational period.

The threshold for SF_4^+ production appears near the onset of the $\tilde{C}$ state of SF_6^+ at 18 eV. Based on this coincidence, and the absence of any apparent influence of the onset of the $\tilde{C}$ state on the SF_5^+, it has long been concluded that the SF_4^+ originates as the exclusive product of the SF_6^+ $\tilde{C}$ state dissociation. [9,14]; Energetically, this is nominally below the threshold for formation of $SF_4^+ + F + F$;, it has been argued that $\tilde{C}$ state dissociation exclusively yields $SF_4^+ + F_2$. Recent calculations show that this appearance energy is actually above the threshold for $SF_4^+ + F + F$ [22]. In fact, the remarkable similarities in the SF_4^+ recoil speed distribution to that of SF_5^+ at lower energy (see Fig. 5) suggest a picture in which the primary product is $SF_5^+ + F$ throughout this region, including the $\tilde{C}$ state. This is supported by the relative insensitivity of the SF_5^+ translational energy distributions to the photon energy, implying that the bulk of the excess energy remains in the SF_5^+ when the photon energy is increased. If it is assumed that the initial step produces SF_5^+ with an average of 0.7 eV translational energy, then secondary decomposition of the SF_5^+ to $SF_4^+ + F$ will become dominant (replacing the SF_5^+ production) at about 18.8 eV. Any residual long-lived SF_5^+ in this region will be found only for the relatively small contribution from the fastest (lowest internal energy) SF_5^+ product. This is precisely what is seen in the PIY curves in Fig. 1; i.e., there is no rise in the SF_5^+ yield in this region.

The angular distributions for SF_4^+ are, within experimental error, isotropic; however, this is difficult to compare directly to SF_5^+ because there is so little new SF_5^+ production at the photon energies where SF_4^+ appears. The absence of anisotropy may simply reflect the difference in the orientation of the electronic transition moment with respect to the bond axis, or it may be a indicator that consequence of the lifetime of the SF_5^+ is long relative to its rotational periodprior to decomposition, or perhaps both. For SF_4^+ at the higher photon energies accessing the $\tilde{E}$ state, however, much of the additional photon energy is coupled effectively into translational energy of the SF_4^+ product. At these higher energies accessing the $\tilde{D}$ and $\tilde{E}$ states, we may be seeing a shift to nonstatistical energy partitioning, or we may have internal conversion to the $\tilde{A}$, $\tilde{B}$ states giving a distinct translational energy distribution for the SF_4^+ product there. Unfortunately, the small yield of new SF_5^+ in the region below the onset of SF_4^+ precludes the use of difference images to probe the threshold behavior there. Clearly, images recorded in coincidence with

true threshold electrons would be very useful to characterize the angular distributions of SF_5^+ near the threshold for secondary decomposition, to provide important confirmation of the proposed origin of SF_4^+ in secondary decomposition of hot SF_5^+.

The SF_3^+ begins to appear around 19 eV, consistent with previous reports. Again for the SF_3^+ however, we see a velocity distribution remarkably similar, at least in the location of the peak, to the SF_5^+ at energies where it is a principal product. The SF_3^+ angular distributions are isotropic, and the velocity distributions change only modestly with photon energy in this region. Fig. 5 shows the SF_3^+ velocity distribution compared to that of SF_4^+ at the same energy. Again, there is an increase as the photon energy is increased, but perhaps the most striking feature of all of these distributions is their similarity. This is consistent with the picture outlined above in which the translational energy release in the primary step, yielding $SF_5^+ + F$, is the principle feature in all of these distributions, and subsequent fluorine atoms are lost sequentially as the energy is available.

The dynamics in the vicinity of the shape resonance are clearly distinct. The preferential production of SF_5^+ and SF_3^+ in that region suggests that autoionization occurs preferentially to lower energy SF_6^+ states leading to SF_5^+ or directly to higher states and near-threshold electrons. Photoelectron spectra recorded on the shape resonance would provide valuable insight into this question.

Acknowledgements

We thank Dr. B. Ruscic for helpful discussions, Mr. D. Chen for assistance in preliminary studies, and acknowledge assistance from the ALS staff. This work was supported by the Director, Office of Energy Research, Office of Basic Energy Sciences, Chemical Sciences Division of the US Department of Energy under Contract No. DE-ACO3-76SF00098. The ALS is supported by the Director, Office of Energy Research, Office of Basic Energy Sciences, Materials Sciences Division of the US Department of Energy under the same contract.

References

[1] Y. Hatano, in: K. Kuchitsu (Ed.), Dynamics of Excited Molecules, Elsevier, 1994, pp. 151–216.
[2] C.Y. Ng, in: C.Y. Ng (Ed.), Vacuum Ultraviolet Photoionization of Photodissociation of Molecules and Clusters, World Scientific, Singapore, 1991, p. 169.
[3] T. Baer, J. Booze, K.M. Weitzel, in: C.Y. Ng (Ed.), Vacuum Ultraviolet Photoionization of Photodissociation of Molecules and Clusters, World Scientific, Singapore, 1991, p. 259.
[4] D.W. Chandler, P.L. Houston, J. Chem. Phys. 87 (1987) 1445.
[5] P.A. Heimann, M. Koike, C.W. Hsu, D. Blank, X.M. Yang, A.G. Suits, Y.T. Lee, M. Evans, C.Y. Ng, C. Flaim, H.A. Padmore, Rev. Sci. Instrum. 68 (1997) 1945.
[6] A.J.R. Heck, D.W. Chandler, Ann. Rev. Phys. Chem. 46 (1995) 335.
[7] S. Hsieh, J.H.D. Eland, Rapid Commun. Mass Spectrom. 9 (1995) 1261.
[8] S. Hsieh, J.H.D. Eland, J. Phys. B 30 (1997) 4515.
[9] J. Berkowitz, Photoabsorption, Photoionzation and Photoelectron Spectroscopy, Academic Press, New York, 1979.
[10] M. Sasanuma, E. Ishiguro, H. Masuko, Y. Morioka, M. Nakamura, J. Phys. B 11 (1975) 3655.
[11] A.P. Hitchcock, M.J.V.d. Viel, J. Phys. B 12 (1979) 2153.
[12] I.G. Simm, C.J. Danby, J.H.D. Eland, P.I. Mansell, J. Chem. Soc. Farad. Trans. II 72 (1976) 426.
[13] K. Mitsuke, S. Suzuki, T. Imamura, I. Koyano, J. Chem. Phys. 93 (1990) 8717.
[14] J.C. Creasey, H.M. Jones, D.M. Smith, R.P. Tuckett, P.A. Hatherly, K. Codling, I. Powis, Chem. Phys. 174 (1993) 441.
[15] M. Evans, C.Y. Ng, C.W. Hsu, P. Heimann, J. Chem. Phys. 106 (1997) 978.
[16] A.J. Yencha, D.B. Thompson, A.J. Cormack, D.R. Cooper, M. Zubek, P. Boloignesi, G.C. King, Chem. Phys. 216 (1997) 227.
[17] J.C. Creasey, I.R. Lambert, R.P. Tuckett, K. Codling, L.J. Frasinski, P.A. Hatherly, M. Stankiewicz, J. Chem. Soc. Faraday Trans. 87 (1991) 1287.
[18] R.N. Zare, Mol. Photochem. 4 (1972) 1.
[19] J.L. Dehmer, J. Chem. Phys. 56 (1972) 4496.
[20] K.-M. Weitzel, C.Y. Ng et al., unpublished results.
[21] Y.S. Cheung, W.K. Li, S.W. Chiu, C.Y. Ng, J. Chem. Phys. 101 (1994) 3412.
[22] Y.S. Cheung, Y.J. Chen, C.Y. Ng, S.W. Chiu, W.K. Li, J. Am. Chem. Soc. 117 (1995) 9725.
[23] K.G. Low, P.D. Hampton, I. Powis, Chem. Phys. 100 (1985) 401.
[24] I. Powis, O. Dutuit, M. Richard-Viard, P.M. Guyon, J. Chem. Phys. 92 (1990) 1643.